0026-895X/08/7306-1659–1667$20.00
MOLECULAR PHARMACOLOGY
Copyright © 2008 The American Society for Pharmacology and Experimental Therapeutics
Mol Pharmacol 73:1659–1667, 2008

Vol. 73, No. 6
41590/3342010
Printed in U.S.A.

A Role for Leu118 of Loop E in Agonist Binding to the α7 Nicotinic Acetylcholine Receptor

Shiva Amiri, Masaru Shimomura, Ranjit Vijayan, Hisashi Nishiwaki, Miki Akamatsu, Kazuhiko Matsuda, Andrew K. Jones, Mark S. P. Sansom, Philip C. Biggin, and David B. Sattelle

Structural Bioinformatics and Computational Biochemistry Unit, Department of Biochemistry (S.A., R.V., M.S.P.S., P.C.B.) and Department of Physiology, Anatomy, and Genetics (A.K.J., D.B.S.), University of Oxford, Oxford, United Kingdom; Department of Applied Biological Chemistry, School of Agriculture, Kinki University, Nara, Japan (M.S., H.N., K.M.); and Graduate School of Agriculture, Kyoto University, Kyoto, Japan (M.A.)

Received September 7, 2007; accepted March 13, 2008

ABSTRACT

Nicotinic acetylcholine receptors (nAChRs) are ligand-gated ion channels mediating fast cholinergic synaptic transmission in the brain and at neuromuscular junctions. We used the structure of the acetylcholine binding protein from *Lymnaea stagnalis* to model the chicken α7 agonist-binding domain. The initial models and a preliminary docking study suggested that position Leu118 may play an important role in determining agonist actions on α7. A prediction from these in silico studies, that L118E and L118D would retain binding to acetylcholine but L118K and L118R would not, was confirmed in electrophysiological studies on functional recombinant mutant receptors expressed in *Xenopus laevis* oocytes. The functional studies also demonstrated that residues at position 118 have a dramatic effect on the actions of imidacloprid (a partial agonist of wild-type α7 receptors) and its des-nitro derivative. Molecular dynamics simulations confirmed that Leu118 can strongly influence agonist binding and that the model was robust in terms of its prediction for acetylcholine binding. Together, the results indicate a role for Leu118 in influencing agonist actions on α7 nAChRs.

Nicotinic acetylcholine receptors (nAChRs) are plasma membrane cation channels activated by the neurotransmitter acetylcholine (ACh). They mediate fast cholinergic synaptic transmission at neuromuscular junctions and in the brain (Léna and Changeux, 1998; Karlin, 2002). The nAChR molecules are pentamers composed of identical or highly homologous subunits, each with four transmembrane regions (1–4) and an extracellular N-terminal domain containing six loops (A–F) that make up the ACh binding site (Corringer et al., 2000). Subunits possessing two adjacent cysteines in loop C of the ACh binding site are designated α subunits, whereas those lacking this cysteine pair are denoted non-α subunits.

Neuronal nicotinic receptor subunits (α2–10; β2–4), which contribute to a variety of receptor subtypes depending on subunit composition (Millar, 2003), are important targets for new drugs (Arneric et al., 2007). These include drugs being developed as analgesics and drugs for ameliorating the symptoms of Alzheimer's disease (Prendergast et al., 1998; Papke et al., 2000), as well as drugs used to treat Parkinson's disease and schizophrenia (Lloyd and Williams, 2000). Congenital myasthenias (Ohno and Engel, 2002) result from mutations in muscle nAChR subunits and autosomal nocturnal frontal lobe epilepsy results from mutations in neuronal α4 and β2 nAChR subunits (Changeux and Edelstein, 2001; Steinlein, 2001). In addition, autoantibodies directed against nAChRs underlie several diseases, such as myasthenia gravis (muscle nAChRs; Lang and Vincent, 2003), Rasmussen's encephalitis (α7; Watson et al., 2005), and autonomic neuropathy (α3; Vernino and Lennon, 2003). The nAChRs of insects are the targets for imidacloprid, a neonicotinoid insecticide extensively used worldwide (Matsuda et al., 2001b). In addition, nematode nAChRs are important targets for

The support of The Medical Research Council of the UK (to A.K.J., D.B.S.) and The Wellcome Trust (to S.A., R.V., M.S.P.S., P.C.B.) is gratefully acknowledged. R.V. thanks the Overseas Research Scheme for support. P.C.B. is an RCUK Fellow. K.M. was supported by the "Academic Frontier" Project for Private Universities from the Ministry of Education, Culture, Sports, Science and Technology of Japan as well as the Integrated Research Project for Plant, Insect, and Animal using Genome Technology from the Ministry of Agriculture, Forestry and Fisheries of Japan. K.M. also acknowledges the support of the program for Basic Research Activities for Innovative Biosciences (Bio-oriented Technology Research Advancement Institution: BRAIN).

S.A. and M.S. contributed equally to this work.

Article, publication date, and citation information can be found at http://molpharm.aspetjournals.org.

doi:10.1124/mol.107.041590.

ABBREVIATIONS: nAChR, Nicotinic acetylcholine receptor; ACh, acetylcholine; AChBP, acetylcholine binding protein; IMI, imidacloprid; DN-IMI, desnitro-imidacloprid; RMSF, root-mean-square fluctuations.

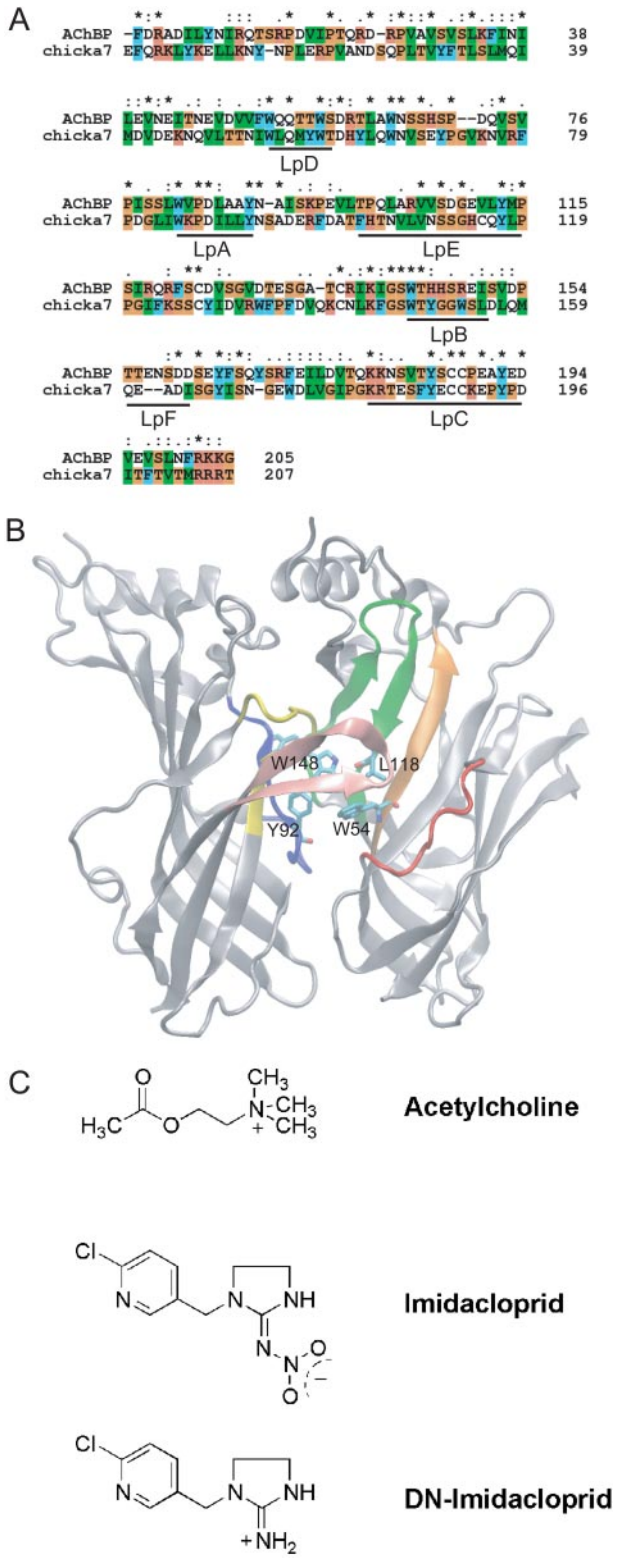

Fig. 1. A, the alignment used with Modeler to generate the initial homology model. The positions of the six loops (loop A–F) involved in ligand binding are indicated. B, only two of the five subunits were used in the docking and simulations runs. The various loops that have been shown to contribute to binding are highlighted: loop A (blue), loop B (yellow), loop C (pink), loop D (orange), loop E (green) and loop F (red). The position Leu118 and other key residues involved in ACh-binding are highlighted in licorice drawing style. C, chemical structures of the ligands used in this study.

anthelmintic drugs such as levamisole, pyrantel, and morantel (Harrow and Gration, 1985; Jones et al., 2005).

The most detailed available structure of a native nAChR in situ has been determined by electron microscopy of tubular crystals of *Torpedo marmorata* postsynaptic membranes embedded in amorphous ice (Miyazawa et al., 1999, 2003; Unwin, 2005). Models based on these coordinates indicate that the extracellular region, containing the ligand-binding site, consists of twisted β-sheets, and loop regions form the binding sites. Brejc et al. (2001) first crystallized a glial-derived acetylcholine binding protein (AChBP) from the freshwater snail *Lymnaea stagnalis*. This 210-amino acid polypeptide forms a stable homopentamer with homology to the N-terminal extracellular region of nAChRs. ACh binding sites are located at each of the five subunit interfaces and the six binding loops (A–F) that can be recognized in nAChRs are also present. Several AChBP crystal structures have now been published (Brejc et al., 2001, 2002; Celie et al., 2004, 2005a,b; Hansen et al., 2005). In view of the important structural homology and sequence similarity (24% identity), between the AChBP and the ligand binding domain of neuronal α7, homology modeling can offer a useful tool to investigate ligand binding. The structure of the chicken α7 homopentamer has been constructed based on both the X-ray structure of the *L. stagnalis* AChBP and the electron microscopy-derived structure of the transmembrane region of the *T. marmorata* nicotinic receptor (Amiri et al., 2005). Le Novère et al. (2002) built a three-dimensional model of the N-terminal domain of a homopentameric chicken α7 nAChR based on AChBP, which was then used to analyze the docking of ACh, epibatidine, and nicotine (Le Novère et al., 2002). Plausible modes of binding were then suggested for these ligands. In a separate modeling study (Schapira et al., 2002), the binding affinities were related to different receptor isotypes. While the manuscript for this article was being written, the crystal structure of the extracellular domain of nAChR α1 subunit bound to α-bungarotoxin at 1.94-Å resolution was solved (Dellisanti et al., 2007). Comparisons between the α1 and AChBP structures suggest that AChBP is indeed a good model for the extracellular ligand-binding domain (Dellisanti et al., 2007).

Photoaffinity labeling studies on the molluscan AChBP showed that Tyr195 in loop C and Met116 of loop E interact with the agonist azidoepibatidine (Tomizawa et al., 2007). Mutagenesis studies have previously shown that the equivalent residue in loop E of vertebrate muscle non-α subunits is involved in ligand binding (Sine, 1997). We have generated homology models of the chicken α7 homopentameric nAChR $(\alpha 7)_5$ and show how in silico methods combined with site-directed mutagenesis yield further evidence that the corresponding loop E residue of α7, Leu118, controls ligand access to the agonist-binding site. We also show that this residue is important in the actions on α7 of the insecticide imidacloprid and its derivative desnitro-imidacloprid.

Materials and Methods

Modeling. A pair-wise sequence alignment for chicken α7 and AChBP (PDB code 1UX2, which has HEPES buffer bound) was generated on the basis of multiple sequence alignments extracted from the pfam database (Bateman et al., 2002) and improved by manual adjustment. The alignment (Fig. 1A) was used as input for the program MODELLER (Sali and Blundell, 1993) to generate 100 initial pentameric models of the chicken α7 ligand binding domain. The quality of the five lowest energy structures was checked with

PROCHECK version 3.5.4 (Laskowski et al., 1993) and the WHAT-IF (http://www.cmbi.kun.nl/gv/servers/WIWWWI) server. The model with the lowest percentage of residues in the disallowed region of the Ramachandran plot was selected for docking studies. Only one binding site from two adjacent subunits was used (see Fig. 1B). In silico site-directed mutagenesis was performed using PyMOL (DeLano, 2004). These structures were deployed as potential docking targets for ACh and imidacloprid using the program Autodock (Morris et al., 1998). Autodock was run with default parameters except that atom types were not set for the ligand but rather according to charges calculated as below. The active site was defined as a radius of (default) 15.0 Å from carbon 6 (IUPAC/IUBMB numbering) of the side chain of Trp148, a residue located centrally in the ACh binding pocket. The charges on ACh were assigned according to a previous report (Segall et al., 1998). Charges for imidacloprid were calculated with the 6–31G* basis set using Spartan (Wavefunction Inc., Irvine, CA). All docking results were visualized with VMD (Humphrey et al., 1996) and UCSF Chimera (Pettersen et al., 2004).

Molecular dynamics simulations were carried out with GROMACS version 3.1.4 (Van der Spoel et al., 2005) using the GROMOS96 (van Gunsteren et al., 1996) force field. Each system was energy-minimized until convergence using a steepest descents algorithm. Molecular dynamics with position restraints for 100 ps was performed followed by equilibration for 1 ns and finally the production run of 10 ns. During the equilibration phase, the temperature and pressure were coupled using the Berendsen methods (Berendsen et al., 1984). During the production runs, the Paranillo-Rahman method (Parinello and Rahman, 1981) was used for pressure coupling, and

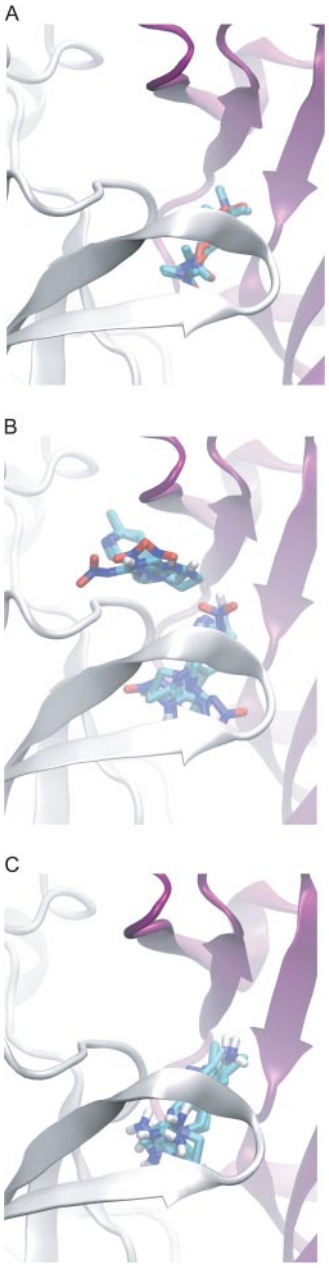

Fig. 2. Lowest energy docking solutions against the wild-type α7 model for ACh (from a total of 4 clusters) (A), for IMI (from 7 clusters with 1.5 kcal/mol of the lowest energy solution) (B), and for DN-IMI (from 6 clusters within 1.5 kcal/mol of lowest energy solution) (C).

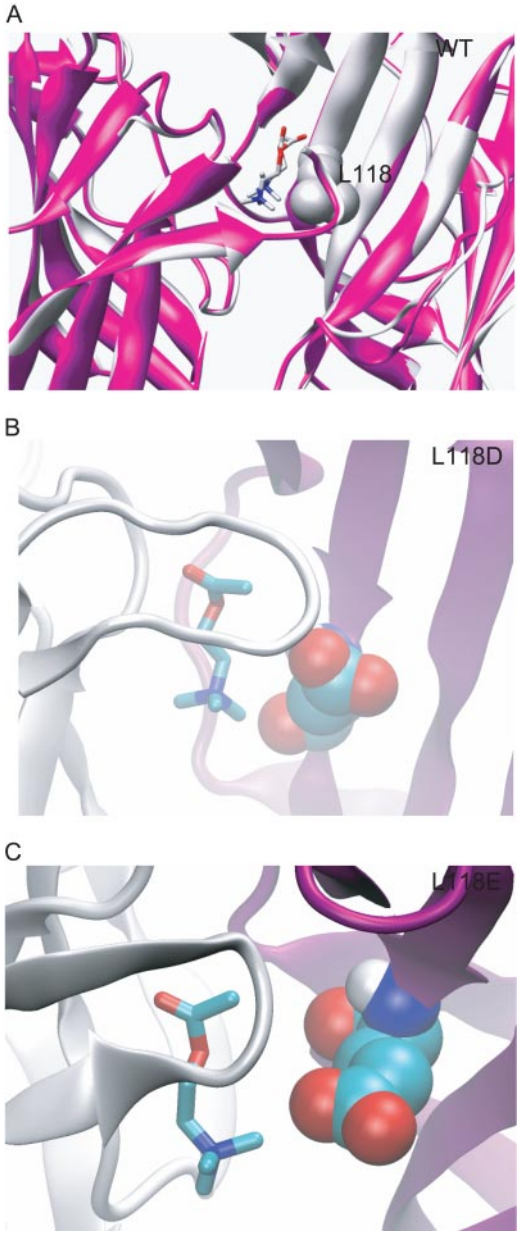

Fig. 3. A, dock of ACh to wild-type α7 model (purple) overlaid onto the AChBP-carbamylcholine structure (1UV6, gray). The position of Leu118 is shown in space fill representation. B, docking of ACh to L118D. The principal subunit is shown in gray and the complimentary subunit is in purple. The D118 residue is shown in space fill and ACh is shown in licorice drawing style. C, docking of ACh to L118E. The Glu118 residue is shown in spacefill. There were no docks in the binding pocket for the L118K and L118R mutations.

the temperature was coupled using the Nosé-Hoover (Nose, 1984) method at 310 K. Electrostatics were calculated with the particle mesh Ewald method (Darden et al., 1993). The LINCS algorithm (Hess et al., 1997) was used to constrain bond lengths, and a time step of 2 fs was used throughout. All calculations were performed on an Intel Pentium III personal computer running Linux kernel 2.4.19smp.

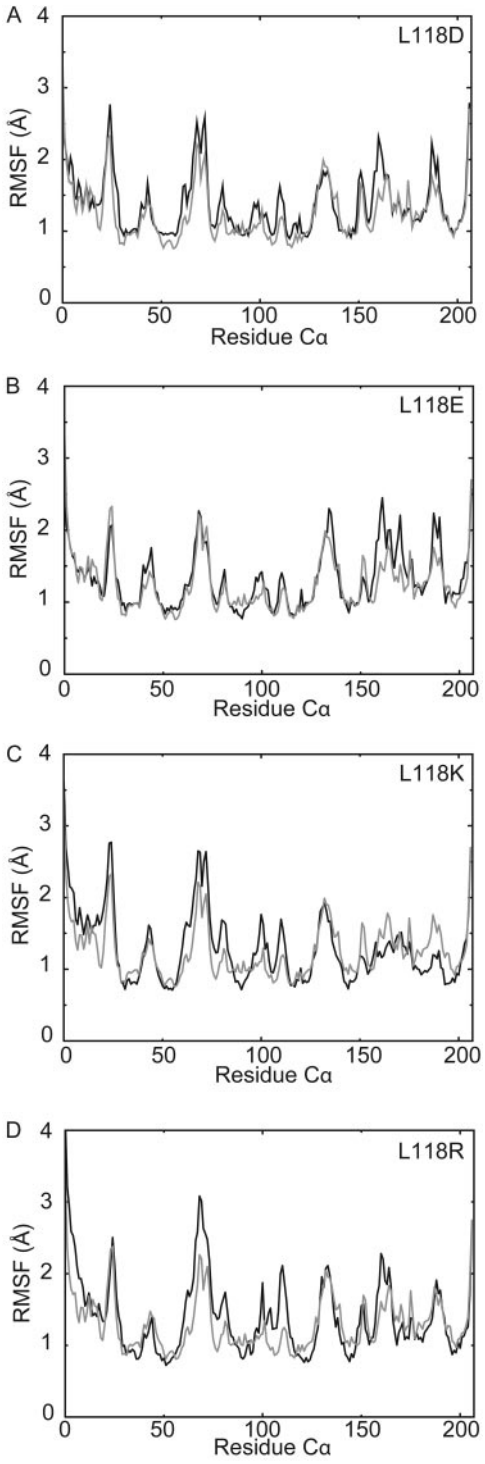

Fig. 4. A, RMSFs of wild type (gray line) compared with the L118D mutation (black line). B, RMSF of wild type (gray line) compared with L118E (black line). C, RMSF of wild type (gray line) compared with L118K (black line). D, RMSF of wild type (gray line) compared with L118R (black line). The mean of all five subunits in each case is plotted.

Electrophysiology on Recombinant Wild-Type and Mutant α7 Receptors. *Xenopus laevis* oocytes were prepared and injected with cDNA (*Gallus gallus* α7 cDNA in pMT3) as described previously (Shimomura et al., 2003). Membrane currents were recorded by the two-electrode voltage-clamp method using 2.0 M KCl-filled electrodes (resistances, 0.5–5.0 MΩ) and a GeneClamp 500B amplifier (Molecular Devices, Sunnyvale, CA). The oocyte membrane was clamped at −100 mV. Oocytes secured in a poly(methyl 2-methylpropenoate) (Perspex) recording chamber (80-μl volume) were perfused continuously at 7 to 10 ml/min by a gravity-fed system with standard oocyte saline composed of 100 mM NaCl, 2.0 mM KCl, 1.8 mM $CaCl_2$, 1.0 mM $MgCl_2$, and 5.0 mM HEPES, pH 7.6. All the test compounds were dissolved in standard oocyte saline and bath-applied to oocytes at intervals of 3 to 5 min to minimize the effects of desensitization. Only oocytes that gave stable responses to two or more successive applications of 200 or 400 μM ACh were used. Concentration-response data were obtained by applying increasing concentrations of agonist to the oocytes. The maximum amplitude of

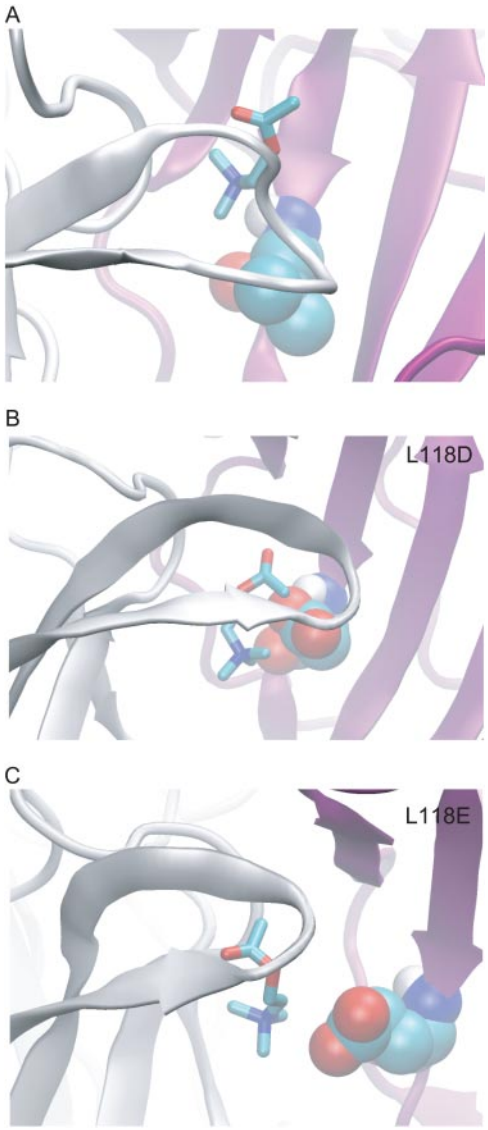

Fig. 5. Docking against snapshots taken from the MD trajectory at 5 ns. Principal subunits are shown in gray and complimentary subunits are shown in purple. A, an example of a dock to snapshot at time = 5 ns for the wild-type. B, an example of a dock to a snapshot at time = 5 ns for the L118D mutation. C, an example of a dock to a snapshot at time = 5 ns for the L118E mutation. The orientation of the docks to these mutants is similar to the solutions found at 0 ns.

the current recorded in response to each application was normalized to the response to 1 mM ACh. As the concentration-response curves for ACh and imidacloprid were changed by the mutations L118D and L118E, data from mutants were normalized using the current response to 3 mM ACh, whereas data from L118K and L118R mutants were normalized using the response to 3 mM imidacloprid. Using Prism software (GraphPad Software, San Diego, CA), normalized data were fitted as described previously (Shimomura et al., 2003).

Binding Assay for Oocyte Membranes Expressing Recombinant Wild-Type and Mutant α7 Receptors. The reaction mixtures (50 μl) containing membrane fraction (2 μg), [^{3}H]ACh (31.25–750 μM), atropine (0.5 μM), and paraoxon (10 μM) were incubated for 1 h at room temperature before the reaction was stopped by filtering through a glass filter GF/C (Whatman International Ltd, Maidstone, England) prewetted with sodium phosphate buffer (10 mM, pH 7.4) containing sodium chloride (50 mM) and polyethylenimine [0.1% (v/v)]. The glass filters were immediately washed with 1.5 ml of sodium phosphate buffer (10 mM, pH 7.4) containing sodium chloride (50 mM), followed by two washes with 5 ml of the same buffer. Each glass filter was then transferred to 3 ml of xylene-based LSCocktail "Aquasol 2" (PerkinElmer Life and Analytical Sciences, Waltham, MA) in a glass vial to measure radioactivity using a liquid scintillation counter (LSC-5100; Aloka Co, Ltd, Tokyo, Japan). Specific binding was defined as the difference of the [^{3}H]ACh binding to the membrane fractions from oocytes expressing recombinant nAChRs and those from vector-injected oocytes. Ligand binding assays were performed in at least triplicate (n = 3–11). The K_d values were calculated from the saturation curves using GraphPad Prism.

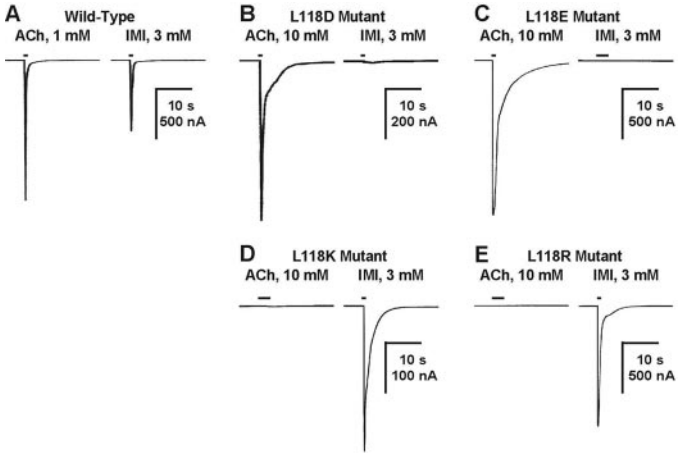

Fig. 6. Maximum current responses of α7 nAChRs to ACh and imidacloprid (IMI). Imidacloprid was a partial agonist, but such an action was completely reduced by L118D (B) and L118E (C) mutations, whereas the ACh-induced response was retained. By contrast, L118K (D) and L118R (E) mutations abolished the response to ACh but not to imidacloprid.

Results

Wild-Type α7 Model. We generated three-dimensional models of the wild-type chicken α7 nAChR. We found that Leu118, which is located in loop E (Corringer et al., 2000), is situated close to the ligand binding site (Fig. 1B) and consequently may influence ligand-protein interactions. We performed docking of ACh, imidacloprid (IMI), and desnitro-imidacloprid (DN-IMI) to the wild-type model. We found that the ACh solutions were tightly clustered (only four clusters) in the binding pocket (Fig. 2A) and spanned an energy range of 0.3 kcal/mol, but for IMI there were several binding modes in a several clusters (Fig. 2B), not all of which were in the immediate binding pocket (7 of 13 clusters were within an energy cut-off of 1.5 kcal/mol of the lowest energy dock). DN-IMI docking also found the binding pocket but several binding modes were again possible with 6 of 9 clusters within an energy cut-off of 1.5 kcal/mol of the lowest energy dock (Fig. 2C). The energies of the IMI and DN-IMI docks were comparable, but all were approximately 3 kcal/mol less than the ACh docks. A comparison of the ACh docking with the crystal structure of carbamylcholine with AChBP (Fig. 3A) revealed that the mode of binding is very similar and thus gave us confidence that the procedure could be used further to predict the interactions of ACh with receptor mutants. However, because the solutions found for IMI and DN-IMI were numerous and there is currently no structural information to confirm the docking solutions, we did not have confidence that the procedure could make reliable predictions for these compounds. Furthermore, there is evidence that the receptor can undergo substantial movement of residues in the binding pocket (Henchman et al., 2003) and, given the size of IMI (and DN-IMI), we reasoned that the pocket may have to undergo substantial movement to accommodate these molecules.

We therefore examined ACh docking to mutant receptors and performed the following in silico mutagenesis on this position; L118E, L118D, L118K, and L118R. The results for ACh docking are shown in Fig. 3; for both the L118D mutation (Fig. 3B) and the L118E mutation (Fig. 3C), the mode of docking resembles that seen for the wild-type receptor (Fig. 3A). There is a slight shift in the position of ACh toward what would be the surface of the membrane in the nAChR molecule. This presumably stems from the increased negative charge at Leu118, which pulls the quaternary nitrogen moiety further downward compared with wild-type. When we tried to dock ACh to the L118K and L118R mutants, we found that ACh would generally not dock into the binding

TABLE 1

I_{max}, pEC_{50}, and Hill coefficient values for acetylcholine, imidacloprid, and desnitro-imidacloprid on wild-type and mutant α7 receptors expressed in *X. laevis* oocytes

Values shown are the result of the concentration-response data (mean ± S.E.M.) shown in Fig. 8. Statistical test (one-way analysis of variance, Dunnett's multiple comparison test) is for significant differences from the wild-type data.

	Acetylcholine				Imidacloprid				Desnitro-Imidacloprid			
	I_{max}	pEC_{50}	Hill	n	I_{max}	pEC_{50}	Hill	n	I_{max}	pEC_{50}	Hill	n
Wild type	1.03 ± 0.04	3.91 ± 0.05	1.4 ± 0.2	5	0.49 ± 0.03	3.63 ± 0.07	1.6 ± 0.4	6	1.21 ± 0.05	5.14 ± 0.07	1.2 ± 0.2	4
L118D	1.07 ± 0.04	2.78 ± 0.04*	1.3 ± 0.2	4	N.D.	N.D.	N.D.	4	1.24 ± 0.11	4.21 ± 0.11*	1.5 ± 0.5	4
L118E	0.97 ± 0.02	3.12 ± 0.03*	1.7 ± 0.2	7	N.D.	N.D.	N.D.	5	1.37 ± 0.06	4.28 ± 0.08*	1.6 ± 0.3	5
L118K	N.D.	N.D.	N.D.	4	1.14 ± 0.10	2.94 ± 0.05*	2.1 ± 0.4	4	N.D.	N.D.	N.D.	4
L118R	N.D.	N.D.	N.D.	5	1.07 ± 0.05	3.00 ± 0.02*	2.4 ± 0.4	5	N.D.	N.D.	N.D.	4

N.D., not determined because the response to agonists were not detected or very small.
* $p < 0.01$

pocket. In the case of L118K, three clusters positioned ACh near the binding pocket but in completely the wrong orientation. The effect was even more marked for the L118R mutation, where not one ACh docking was even in the binding pocket. These studies suggested that negatively charged mutations at this position would retain ACh binding, but positively charged mutations would impair ACh binding.

Molecular Dynamics and Multiple Docking. Before embarking on experiments to confirm these predictions, we decided to examine how robust the homology models were to local fluctuations. We were also interested in exploring the consequence of mutations on the stability of the structure. Ten-nanosecond molecular dynamics (MD) simulations for the wild-type and mutant α7 subunits were therefore performed. A common method for analyzing the relative stability of protein simulations is to analyze the root-mean-square fluctuations (RMSF) of the Cα atoms. Analysis of the RMSF for AChBP molecules revealed that the mutant structures showed a higher mean RMSF (Fig. 4, A–D), indicating that this residue has a large influence on the dynamics of the protein. In particular, the regions corresponding to loop E (residues 112–119) appear to exhibit larger fluctuations compared with wild-type. In the case of L118D and L118E, there are also increased fluctuations for loop C.

Because the result of an MD simulation is to produce a series of coordinates versus time, this presents a means to test the model and the sensitivity of the docking of ACh with respect to local fluctuations of the model. To do this, we took 100 snapshots from the simulation, one every 100 ps. We then docked ACh back into these snapshots to assess how well the binding pocket retained its shape and ability to accommodate ACh. This analysis showed that the results observed for the starting model were maintained throughout the simulation (see typical snapshots taken from frames at 5 ns in Fig. 5, A–C), suggesting that small, local residue fluctuations were not critical in determining the pattern of binding. Docking of ACh to snapshots from the wild-type, L118D, and L118E resulted in solutions that were both in the binding pocket and had an orientation consistent with carbamylcholine bound to AChBP (Celie et al., 2004). Conversely, L118K and L118R mutant models failed to produce docking solutions with ACh in the binding pocket. Thus, results from the in silico study suggested that the negatively charged mutations (L118D and L118E) would retain the ability to bind ACh, but the positively charged mutations (L118K and L118R) would not.

Electrophysiological Studies on Wild-Type and Leu118-Mutated α7 nAChRss. We investigated the effects of L118D, L118E, L118K, and L118R substitutions on the functional α7 nAChR expressed in *X. laevis* oocytes. Control experiments on wild-type α7 show that imidacloprid is a partial agonist (Fig. 6A) consistent with earlier experiments (Matsuda et al., 2000). Figure 6 shows that after the L118D and L118E mutations, responses of the α7 receptor to imidacloprid were abolished ($P < 0.01$ using a one-way ANOVA Dunnett's multiple comparison test). However, the α7 mutants still responded to ACh (Fig. 6, B and C). The EC_{50} values of ACh were increased by these two mutations (Table 1). In complete contrast to the findings for the L118D and L118E mutations, L118K and L118R mutations blocked the responses to ACh, whereas responses to imidacloprid were observed (Fig. 6, D and E). In addition to these striking effects on the responses to ACh and imidacloprid, the mutations of Leu118 slowed the desensitization of the responses.

DN-IMI is a derivative of imidacloprid lacking the nitro group. The guanidine moiety of this compound is protonated at neutral pH (Fig. 1C). The maximum response to DN-IMI of the wild-type α7 nAChR expressed in *X. laevis* oocytes was slightly greater than the response to ACh (Fig. 7A), resembling results of a previous study (Ihara et al., 2003). The L118D and L118E mutations did not significantly affect the maximum response of α7 to DN-IMI (Fig. 7, B and C) (Table 1). However, the concentration-response curve of DN-IMI was shifted to the right by the L118D and L118E mutations (Table 1). In contrast to the effects on the maximum response to imidacloprid, the L118K and L118R mutations abolished the nicotinic receptor response to DN-IMI (Fig. 7, D and E). Thus the pEC_{50} values for DN-IMI could not be determined for these two mutant receptors.

The concentration-response curves of ACh, imidacloprid and DN-IMI for the wild-type (A) and L118D (B), L118E (C), L118K (D), and L118E (E) mutants are shown in Fig. 8. It could be argued that, in certain mutants, imidacloprid may antagonize the response to ACh and ACh may antagonize the actions of imidacloprid. To begin to address this, we have examined whether the response to imidacloprid of the L118R mutant and, similarly, the response to ACh of the L118D mutant are suppressed by coapplication with ACh and imidacloprid, respectively. It was found that the response to 1 mM imidaclolprid in loop E was suppressed by coapplication with 1 mM ACh to 0.306 ± 0.099 ($n = 2$) compared with the response (= 1.00) to 1 mM imidaclolprid alone. On the other hand, the response to 3 mM ACh of the L118D mutant was suppressed by coapplication with 1 mM imidacloprid to 0.721 ± 0.125 ($n = 2$) compared with the response (= 1.00) to 3 mM ACh alone.

Radioligand Binding Studies on Wild-Type and Mutant α7 nAChRs. Binding experiments were also conducted to evaluate the affinity of [^{3}H]ACh for the oocyte membrane fractions including the recombinant wild type and mutant α7 nAChRs. [^{3}H]ACh showed saturable binding to the membrane fractions (Fig. 9). The K_d values (mean ± S.E.M.) of ACh for the wild type, L118R, and L118D were 211.4 ± 56.9,

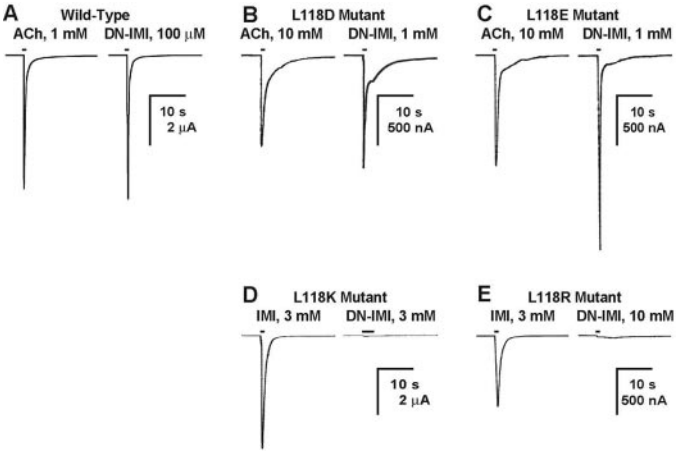

Fig. 7. Maximum current responses of α7 nAChRs to ACh and DN-IMI. DN-IMI induced similar current amplitude of the maximum response to ACh of the wild-type nicotinic receptor (A). L118D (B) and L118E (C) mutations retained the DN-IMI-induced response, whereas L118K (D) and L118R (E) mutations markedly reduced it.

538.6 ± 285.1, and 109.5 ± 64.1 μM, respectively. The K_d value of [^{3}H]imidaclolprid could not be determined because of its low binding affinity (data not shown).

Discussion

Our prediction of ACh-nAChR interaction for several mutants at position Leu118 of α7 is supported by the in vitro experiments, suggesting that this model is capable of capturing the effects of ACh interacting with homomeric α7 nAChRs. A previous report also highlights the involvement of the corresponding residue in ligand binding, where L119C, L119C, and L121C mutants of the vertebrate muscle nAChR subunits γ, ε, and δ, respectively, treated with aminoethyl methanethiosulfonate showed reduced affinity for dimethyl-*d*-tubocurarine and α-conotoxin M1 (Sine, 1997). Similar results were observed for the γL119K, εL119K, and δL121K mutants. In addition, using photoaffinity labeling, a methionine (Met116) at the equivalent position in loop E of another molluscan AChBP from *Aplysia californica* was shown to be involved in imidacloprid binding (Tomizawa et al., 2007). All of these findings indicate that the pyridine ring of imidacloprid is likely to interact with loop E, placing its nitro group so as to interact with other residues facing the agonist binding domain.

Several studies have shown that electrostatic forces are important for imidacloprid interaction with nAChRs (Sattelle et al., 2005; Ihara et al., 2007). Here we show that substitutions of Leu118 in loop E by acidic or basic residues strikingly influence the responses of α7 to ACh. It should be noted that the antagonist action of ACh on the response of the L118D mutant to 1 mM imidacloprid was not sufficiently potent to block the response completely. A possible simple explanation for the effects of such mutations is that if Leu118 were mutated to a positive side-chain, the interaction with the charged quaternary nitrogen might be strong enough to prevent binding to the pocket; as a result, the channel fails to open. We have confidence that our model of $(\alpha7)_5$ is reasonable because an orientation of ACh similar to that found for carbamylcholine in AChBP (Celie et al., 2004) was predicted. Furthermore, our model seems robust to small local changes in residue conformation as exemplified by the molecular dynamics (Fig. 4). In addition, the recent structure of the α1 nAChR subunit ligand-binding domain (Dellisanti et al., 2007) suggests that AChBP provides a suitable template for modeling the extracellular domain in this way.

Our initial model did not allow us to make confident predictions about the interactions of imidacloprid with the $(\alpha7)_5$ model. This is perhaps not too surprising given that our model is based upon AChBP with HEPES bound. If the receptor conforms to an induced-fit model in terms of its interactions with ligands, then the model will suffer from being biased away from a conformation that would bind imidacloprid. Furthermore, recent experiments on AChBP (Gao et al., 2005) and on homology models of α7 (Henchman et al., 2003, 2005) suggest that there can be substantial changes in the shape of the binding pocket, in particular the conformation of loop C.

However, taking all these factors into consideration along with our present findings, we propose a model that accounts for the data shown in Figs. 6 and 7. Imidacloprid has a negatively charged nitro group, whereas DN-IMI possesses a positive charge at the guanidine moiety. It is interesting to note that the effects of mutations on DN-IMI are quite similar to those seen for ACh. Thus it could be that the positions of their positive charges in the binding pocket are similar.

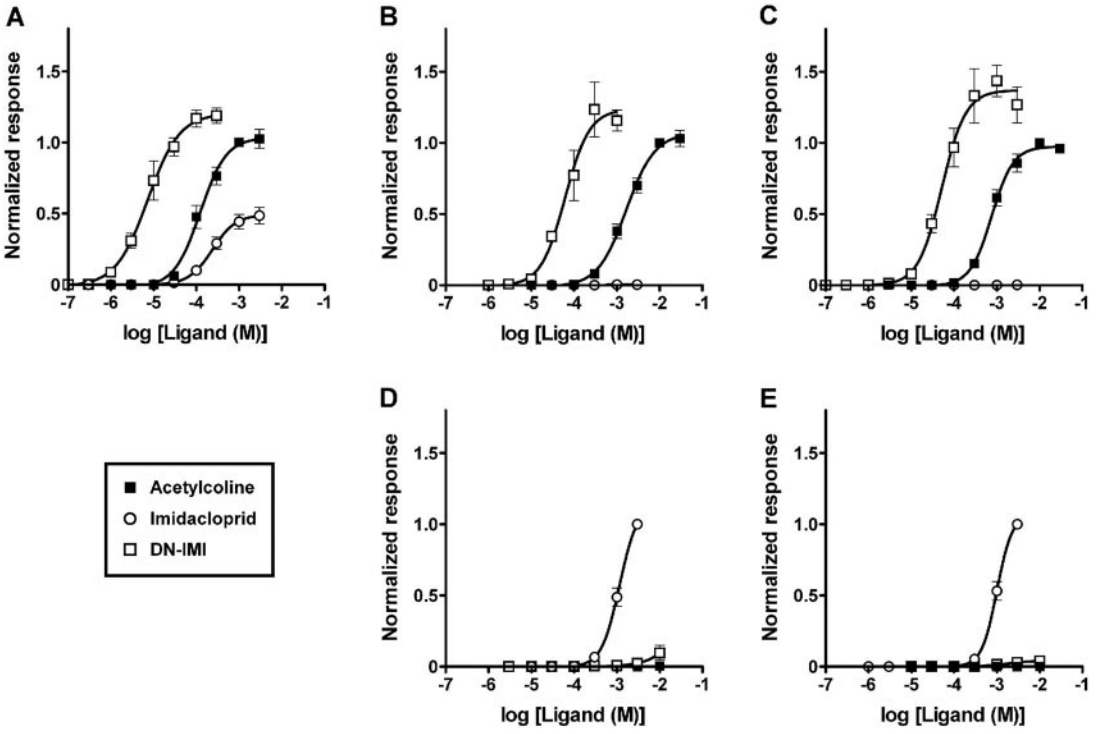

Fig. 8. Concentration-response curves of ACh, imidacloprid, and DN-IMI obtained for wild-type (A), as well as L118D (B), L118E (C), L118K (D), and L118R (E) mutants of the α7 nAChR expressed in *X. laevis* oocytes. Each plot represents mean ± S.E.M. of 4 to 7 experiments using at least two different batches of eggs.

However, that would presumably require a different conformation of loop C to allow the DN-IMI to adopt a sterically favorable position within the binding pocket. Imidacloprid itself fails to generate currents in L118D and L118E mutants, but can effect channel opening in the case of L118K and L118R mutants. However, imidacloprid modulated the ACh-induced response of the L118D mutant, suggesting that the electrostatic interaction between the nitro group and this residue is critical in determining whether it will permit channel opening in response to agonist binding. A similar explanation is possible for the action of ACh on the mutant receptors. The Leu118 mutations influenced the desensitization of the imidacloprid- and ACh-induced responses, reflecting the role for Leu118 in the channel gating mechanism.

Electrostatic interactions are not the only forces determining agonist interactions with the α7 nAChR. The L118D and L118E mutations shifted the ACh concentration-response curve to higher concentrations and slightly reduced the maximum current amplitudes observed in response to ACh (Fig. 8), suggesting that such mutations in loop E may lead indirectly to a conformational change in another region of the receptor playing a key role in interactions with agonists.

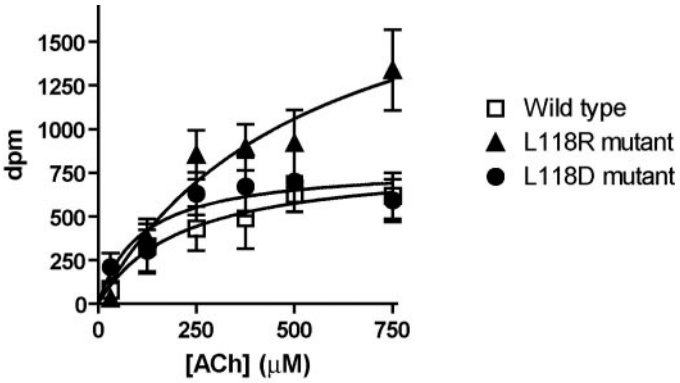

Fig. 9. Saturation curve for [^{3}H]acetylcholine binding to *X. laevis* oocyte membranes expressing the wild-type and L118R and L118D mutant α7 nicotinic acetylcholine receptors. Each point plotted represents the mean with the S.E.M. shown (n = 3–11).

TABLE 2
Amino acid sequences in loop E
The residues corresponding to L118 of chicken α7 are underlined and basic residues at this position are shown in bold.

nAChR Subunit	Loop E Sequence
L. stagnalis AChBP	GEVLYMPSIRQ
Chicken α7	GHCQYLPPGIF
Chicken α4	GRIKWMPPAIY
Chicken β2	GSIFWLPPAIY
Rat β2	GSIFWLPPAIY
Rat β4	GSIQWLPPAIY
D. melanogaster α1 (ALS)	GKVVW**K**PPAIY
D. melanogaster α2 (SAD)	GKVVWTPPAIF
D. melanogaster α3	GRVEW**R**PPAIY
D. melanogaster α4	GLVEW**K**PPAIY
D. melanogaster α5	GSCLYVPPGIF
D. melanogaster α6	GSCLYVPPGIF
D. melanogaster α7	GSCLYVPPGIF
D. melanogaster β1 (ARD)	GEVLWVPPAIY
D. melanogaster β2 (SBD)	GEVFWEPPAIY
D. melanogaster β3	GHFRWMPPAVY
M. persicae α1	GKVMWTPPAIY
M. persicae α2	GKVVW**K**PPAIY
M. persicae α3	GRVEW**K**PPAIY
M. persicae α4	GEVLWSPPAIY

Thus, it will be necessary to further improve the modeling to gain a more complete understanding of neonicotinoid-nAChR interactions. Nevertheless, electrostatic interactions can explain the changes in concentration-response curves of the imidacloprid derivative DM-IMI lacking the nitro group. Unlike imidacloprid, DN-IMI has a positive charge at the guanidine moiety, thereby mimicking ACh. Consistent with this, the L118K and L118R mutations abolished responses of the α7 nAChR to DN-IMI, whereas L118D and L118E mutations permitted the agonist actions of this ligand.

Leu118 is not highly conserved across the nAChR family. Thus, the residue at this location may participate in determining subunit-specific responses to agonists. In the *Drosophila melanogaster* Dβ2 subunit, the residue corresponding to Leu118 is glutamic acid (Table 2). Because we found that the L118E mutation in α7 abolished imidacloprid action but retained sensitivity to ACh, it is predicable that imidacloprid will not be efficacious on insect nAChRs containing Dβ2 subunit in opening the channel gate. Conversely, several other insect nAChR subunits, such as *D. melanogaster* Dα1, Dα3, and Dα4, as well as *Myzus persicae* α2 and α3, possess either an arginine or lysine at the position corresponding to Leu118 (Table 2), which in our site-directed mutagenesis experiments increased the efficacy of imidacloprid (Table 1). It is noteworthy that studies have indicated that these subunits play a role in determining sensitivity to the insecticide, imidacloprid (Huang et al., 1999; Lansdell and Millar, 2000; Matsuda et al., 2001a; Shimomura et al., 2002, 2003, 2004, 2006). In heteromeric nAChRs consisting of α and β subunits, it is believed that loop E from the β subunit contributes to the agonist binding site (Corringer et al., 2000b); however, it is important to note that the subunit composition and stoichiometry of native insect nAChRs have yet to be determined. Such information will prove instructive in assessing the relevance of loops A to F of either α or β subunits in agonist binding and hence neonicotinoid sensitivity. In addition, mutations at Leu118 may provide a route by which target-site resistance could develop. If it is the case that in several insect nAChR α subunits, the arginine or lysine at the residue corresponding to Leu118 contributes to imidacloprid sensitivity, a simple negative charge mutation here would be enough to maintain responses to the natural agonist, ACh, while abolishing the agonist actions of imidacloprid. Thus in searching field strains resistant to imidacloprid, it may be of interest to look for changes in loop E as well as the important loop B mutations (Liu et al., 2005) already known to be associated with imidacloprid resistance.

In conclusion, we have used molecular modeling to predict that Leu118 of the α7 nAChR subunit contributes to agonist binding. Site-directed mutagenesis and functional expression of wild-type and mutant nAChRs subsequently confirmed this prediction. These results, taken together with our previous studies on loops C, D, and F (Shimomura et al., 2002, 2003, 2004, 2006), enhance our understanding of the binding to nAChRs of commercially important nicotinic agonists.

Acknowledgments

We thank M. Ballivet (Department of Biochemistry, University of Geneva, Switzerland) for kindly providing the chicken α7 cDNA.

References

Amiri S, Tai K, Beckstein O, Biggin PC, and Sansom MS (2005) The α7 nicotinic acetylcholine receptor: molecular modelling, electrostatics, and energetics. *Mol Membr Biol* **22:**151–162.

Arneric SP, Holladay M, and Williams M (2007) Neuronal nicotinic receptors: a perspective on two decades of drug discovery research. *Biochem Pharmacol* **74:** 1092–1101.

Bateman A, Birney E, Cerruti L, Durbin R, Etwiller L, Eddy SR, Griffiths-Jones S, Howe KL, Marshall M, and Sonnhammer EEL (2002) The pfam protein families database. *Nucleic Acids Res* **30:**276–280.

Berendsen HJC, Postma JPM, van Gunsteren WF, DiNola A, and Haak JR (1984) Molecular dynamics with coupling to an external bath. *J Chem Phys* **81:**3684–3690.

Brejc K, van Dijk WJ, Klassen RV, Schuurmans M, van Der Oost J, Smit AB, and Sixma TK (2001) Crystal structure of an ACh-binding protein reveals the ligand-binding domain of nicotinic receptors. *Nature* **411:**269–276.

Brejc K, van Dijk WJ, Smit AB, and Sixma TK (2002) The 2.7 Å structure of AChBP, homologue of the ligand-binding domain of the nicotinic acetylcholine receptor. *Novartis Found Symp* **245:**22–29.

Celie PH, Kasheverov IE, Mordvintsev DY, Hogg RC, van Nierop P, van Elk R, van Rossum-Fikkert SH, Zhmak MN, Bertrand D, Tsetlin V, et al. (2005a) Crystal structure of nicotinic acetylcholine receptor homolog AChBP in complex with an α-conotoxin PnIA variant. *Nat Struct Mol Biol* **12:**582–588.

Celie PH, Klassen RV, van Rossum-Fikkert SH, van Elk R, van Nierop P, Smit AB, and Sixma TK (2005b) Crystal structure of acetylcholine-binding protein from *Bulinus truncatus* reveals the conserved structural scaffold and sites of variation in nicotinic acetylcholine receptors. *J Biol Chem* **280:**26457–26466.

Celie PH, van Rossum-Fikkert SE, van Dijk WJ, Brejc K, Smit AB, and Sixma TK (2004) Nicotine and carbamylcholine binding to nicotinic acetylcholine receptors as studied in AChBP crystal structures. *Neuron* **41:**907–914.

Changeux JP and Edelstein SJ (2001) Allosteric mechanisms in normal and pathological nicotinic acetylcholine receptors. *Curr Opin Neurobiol* **11:**369–377.

Corringer PJ, Le Novère N, and Changeux J-P (2000) Nicotinic receptors at the amino acid level. *Annu Rev Pharmacol Toxicol* **40:**431–458.

Darden T, York D, and Pedersen L (1993) Particle mesh Ewald - an N.log(N) method for Ewald sums in large systems. *J Chem Phys* **98:**10089–10092.

DeLano WL (2004) The PyMOL molecular graphics system. DeLano Scientific LLC, San Carlos, CA.

Dellisanti CD, Yao Y, Stroud JC, Wang ZZ, and Chen L (2007) Crystal structure of the extracellular domain of nAChR α1 bound to α-bungarotoxin at 1.94 A resolution. *Nat Neurosci* **10:**953–962.

Gao F, Bren N, Burghardt TP, Hansen SB, Henchman RH, Taylor P, McCammon JA, and Sine SM (2005) Agonist-mediated conformational changes in acetylcholine-binding potein revealed by simulation and intrinsic tryptophan fluorescence. *J Biol Chem* **280:**8443–8451.

Hansen SB, Sulzenbacher G, Huxford T, Marchot P, Taylor P, and Bourne Y (2005) Structures of the *Aplysia* AChBP complexes with nicotinic agonists and antagonists reveal distinctive binding interfaces and conformations. *EMBO J* **24:**3635–3646.

Harrow ID and Gration KAF (1985) Mode of action of the anthelmintics morantel, pyrantel and levimisole on muscle cell membrane of the nematode *Ascatis suum*. *Pesti Sci* **16:**662–672.

Henchman RH, Wang HL, Sine SM, Taylor P, and McCammon JA (2003) Asymmetric structural motions of the homomeric a7 nicotinic receptor ligand binding domain revealed by molecular dynamics simulation. *Biophys J* **85:**3007–3018.

Henchman RH, Wang HL, Sine SM, Taylor P, and McCammon JA (2005) Ligand-induced conformational change in the alpha7 nicotinic receptor ligand binding domain. *Biophys J* **88:**2564–2576.

Hess B, Bekker J, Berendsen HJ, and Fraaije JG (1997) LINCS: A linear constraint solver for molecular simulations. *J Comput Chem* **18:**1463–1472.

Huang Y, Williamson MS, Devonshire AL, Windass JD, Lansdell SJ, and Millar NS (1999) Molecular characterization and imidacloprid selectivity of nicotinic acetylcholine receptor subunits from the peach-potato aphid *Myzus persicae*. *J Neurochem* **73:**380–389.

Humphrey W, Dalke A, and Schulten K (1996) VMD: visual molecular dynamics. *J Mol Graph* **14:**33–38.

Ihara M, Matsuda K, Otake M, Kuwamura M, Shimomura M, Komai K, Akamatsu M, Raymond V, and Sattelle DB (2003) Diverse actions of neonicotinoids on chicken α7, $\alpha4\beta2$ and *Drosophila*-chicken SADβ2 and ALSβ2 hybrid nicotinic acetylcholine receptors expressed in *Xenopus laevis* oocytes. *Neuropharmacology* **45:**133–144.

Ihara M, Shimomura M, Ishida C, Nishiwaki H, Akamatsu M, Sattelle DB, and Matsuda K (2007) A hypothesis to account for the selective and diverse actions of neonicotinoid insecticides at their molecular targets, nicotinic acetylcholine receptors: catch and release in hydrogen bond networks. *Invert Neurosci* **7:**47–51.

Jones AK, Buckingham SD, and Sattelle BM (2005) Chemistry-to-gene screens in *Caenorhabditis elegans*. *Nat Rev Drug Discov* **4:**321–330.

Karlin A (2002) Emerging structure of the nicotinic acetylcholine receptors. *Nat Rev Neurosci* **3:**102–114.

Lang B and Vincent A (2003) Autoantibodies to ion channels at the neuromuscular junction. *Autoimmun Rev* **2:**94–100.

Lansdell SJ and Millar NS (2000) The influence of nicotinic receptor subunit composition upon agonist, alpha-bungarotoxin and insecticide (imidacloprid) binding affinity. *Neuropharmacology* **39:**671–679.

Laskowski RA, Macarthur MW, Moss DS, and Thornton JM (1993) PROCHECK: A program to check the stereochemical quality of protein structures. *J Appl Crystallogr* **26:**283–291.

Le Novère N, Grutter T, and Changeux J-P (2002) Models of the extracellular domain of the nicotinic receptors and of agonist- and Ca^{2+}-binding sites. *Proc Natl Acad Sci U S A* **99:**3210–3215.

Léna C and Changeux J-P (1998) Allosteric nicotinic receptors, human pathologies. *J Physiol Paris* **92:**63–74.

Liu Z, Williamson MS, Lansdell SJ, Denholm I, Han Z, and Millar NS (2005) A nicotinic acetylcholine receptor mutation conferring target-site resistance to imidacloprid in *Nilaparvata lugens* (brown planthopper). *Proc Natl Acad Sci U S A* **102:**8420–8425.

Lloyd GK and Williams M (2000) Neuronal nicotinic acetylcholine receptors as novel drug targets. *J Pharmacol Exp Ther* **292:**461–467.

Matsuda K, Buckingham SD, Kleier D, Rauh JJ, Grauso M, and Sattelle DB (2001a) Neonicotinoids: insecticides acting on insect nicotinic acetylcholine receptors. *Trends Pharmacol Sci* **22:**573–580.

Matsuda K, Ihara M, Nishimura K, Sattelle DB, and Komai K (2001b) Insecticidal and neural activities of candidate photoaffinity probes for neonicotinoid binding sites. *Biosci Biotechnol Biochem* **65:**1534–1541.

Matsuda K, Shimomura M, Kondo Y, Ihara M, Hashigami K, Yoshida M, Raymond V, Mongan NP, Freeman JC, Komai K, et al. (2000) Role of loop D of the α7 nicotinic acetylcholine receptor in its interaction with the insecticide imidacloprid and related neonicotinoids. *Br J Pharmacol* **130:**981–986.

Millar NS (2003) Assembly and subunit diversity of nicotinic acetylcholine receptors. *Biochem Soc Trans* **31:**869–874.

Miyazawa A, Fujiyoshi Y, Stowell M, and Unwin N (1999) Nicotinic acetylcholine receptor at 4.6 Å resolution: transverse tunnels in the channel wall. *J Mol Biol* **288:**765–786.

Miyazawa A, Fujiyoshi Y, and Unwin N (2003) Structure and gating mechanism of the acetylcholine receptor pore. *Nature* **423:**949–955.

Morris GM, Goodsell DS, Halliday RS, Huey R, Hart WE, Belew RK, and Olson AJ (1998) Automated docking using a Lamarckian genetic algorithm and an empirical binding free energy function. *J Comput Chem* **19:**1639–1662.

Nose S (1984) A molecular dynamics method for simulations in the canonical ensemble. *Mol Phys* **52:**255–268.

Ohno K and Engel AG (2002) Congenital myasthenic syndromes: genetic defects of the neuromuscular junction. *Curr Neurol Neurosci Rep* **2:**78–88.

Papke RL, Meyer E, Nutter T, and Uteshev VV (2000) α7 receptor-selective agonists and modes of α7 receptor activation. *Eur J Pharmacol* **393:**179–195.

Parinello M and Rahman A (1981) Polymorphic transitions in single crystals—a new molecular dynamics method. *J Appl Phys* **52:**7182–7190.

Pettersen EF, Goddard TD, Huang CC, Couch GS, Greenblatt DM, Meng EC, and Ferrin TE (2004) USCF chimera—a visualization system for exploratory research and analysis. *J Comput Chem* **25:**1605–1612.

Prendergast MA, Jackson WJ, Terry AVJ, Decker MW, Arneric SP, and Buccafusco JJ (1998) Central nicotinic receptor agonists ABT-418, ABT-089, and (−)-nicotine reduce distractibility in adult monkeys. *Psychopharmacology (Berl)* **136:**50–58.

Sali A and Blundell TL (1993) Comparative protein modelling by satisfaction of spatial restraints. *J Mol Biol* **234:**779–815.

Sattelle DB, Jones AK, Sattelle BM, Matsuda K, Reenan R, and Biggin PC (2005) Edit, cut and paste in the nicotinic acetylcholine receptor gene family of *Drosophila melanogaster*. *Bioessays* **27:**366–376.

Schapira M, Abagyan R, and Totrov M (2002) Structural model of nicotinic acetylcholine receptor isotypes bound to acetylcholine and nicotine. *BMC Struct Biol* **2:**1–8.

Segall MD, Payne MC, and Boyes RN (1998) An ab initio study of the conformational energy map of acetylcholine. *Mol Phys* **93:**365–370.

Shimomura M, Okuda H, Matsuda K, Komai K, Akamatsu M, and Sattelle DB (2002) Effects of mutations of a glutamine residue in loop D of the α7 nicotinic acetylcholine receptor on agonist profiles for neonicotinoid insecticides and related ligands. *Br J Pharmacol* **137:**162–169.

Shimomura M, Yokota M, Ihara M, Akamatsu M, Sattelle DB, and Matsuda K (2006) Role in the selectivity of neonicotinoids of insect-specific basic residues in loop D of the nicotinic acetylcholine receptor agonist binding site. *Mol Pharmacol* **70:**1255–1263.

Shimomura M, Yokota M, Matsuda K, Sattelle DB, and Komai K (2004) Roles of loop C and the loop B-C interval of the nicotinic receptor α subunit in its selective interactions with imidacloprid in insects. *Neurosci Lett* **363:**195–198.

Shimomura M, Yokota M, Okumura M, Matsuda K, Akamatsu M, Sattelle DB, and Komai K (2003) Combinatorial mutations in loops D and F strongly influence responses of the α7 nicotinic acetylcholine receptor to imidacloprid. *Brain Research* **991:**71–77.

Sine SM (1997) Identification of equivalent residues in the γ, δ, and ε subunits of the nicotinic receptor that contribute to α-bungarotoxin binding. *J Biol Chem* **272:** 23521–23527.

Steinlein OK (2001) Genes and mutations in idiopathic epilepsy. *Am J Med Genet* **106:**139–145.

Tomizawa M, Maltby D, Medzihradszky KF, Zhang N, Durkin KA, Presley J, Talley TT, Taylor P, Burlingame AL, and Casida JE (2007) Defining nicotinic agonist binding surfaces through photoaffinity labeling. *Biochemistry* **46:**8798–8806.

Unwin N (2005) Refined structure of the nicotinic acetylcholine receptor at 4Å resolution. *J Mol Biol* **346:**967–989.

Van Der Spoel D, Lindahl E, Hess B, Groenhof G, Mark AE, and Berendsen HJ (2005) GROMACS: fast, flexible, and free. *J Comput Chem* **26:**1701–1718.

van Gunsteren WF, Krüger P, Billeter SR, Mark AE, Eising AA, Scott WRP, Hüneberger PH, and Tironi IG (1996) Biomolecular simulation: the GROMOS96 manual and user guide, Biomos/Hochschulverlag AG an der ETH Zürich, Groningen/Zürich.

Vernino S and Lennon VA (2003) Neuronal ganglionic acetylcholine receptor autoimmunity. *Ann N Y Acad Sci* **998:**211–214.

Watson R, Jepson JE, Bermudez I, Alexander S, Hart Y, McKnight K, Roubertie A, Fecto F, Valmier J, Sattelle DB, et al. (2005) α7-acetylcholine receptor antibodies in two patients with Rasmussen encephalitis. *Neurology* **65:**1802–1804.

Address correspondence to: David B. Sattelle, University of Oxford, South Parks Road, Oxford OX1 3QX, UK. E-mail: david.sattelle@anat.ox.ac.uk